

Paper:

Gait Rehabilitation System Using a Non-Wearing Type Pneumatic Power Assist Device

Masashi Yokota* and Masahiro Takaiwa**

*Graduate School Advanced Technology and Science, Tokushima University
2-1 Minamijyousanjima-cho, Tokushima 770-8506, Japan
E-mail: c501942002@tokushima-u.ac.jp

**Graduate School of Technology, Industrial and Social Sciences, Tokushima University
2-1 Minamijyousanjima-cho, Tokushima 770-8506, Japan

[Received June 8, 2021; accepted July 12, 2021]

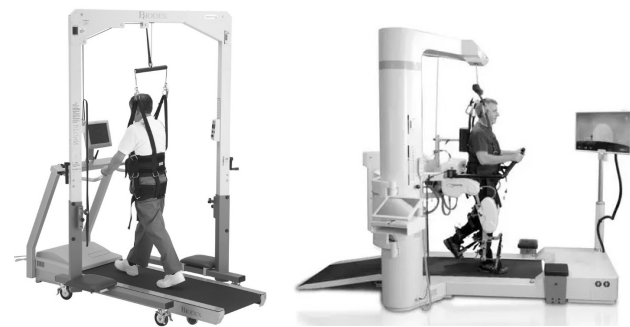
In Japan, approximately 1.1 million people suffer from cerebrovascular diseases such as cerebral stroke, which can further increase due to the aging society. Therefore, rehabilitation for the physical recovery of patients with hemiplegia caused by cerebrovascular disease plays an important role in maintaining and improving their quality of life (QoL). In rehabilitation facilities, crutches and parallel bars are the mainstream, but patients support their body with their arms, causing falls and fatigue, leading to deterioration of motivation in long-term rehabilitation. Although a few hanging-type devices have been developed to cope with such issues, they occupy large space, require time to wear, and have a high introduction cost. In this study, we developed a non-wearing-type pneumatic power assist device for gait rehabilitation to ensure patients can sustain their body weight by pushing up their armpit and quantitatively verified the effectiveness of the device.

Keywords: pneumatic drive, power assist, non-wearing type, force control, disturbance observer

1. Introduction

According to an annual report by the Ministry of Health, Labor and Welfare, Japan, the number of patients with cerebrovascular diseases such as cerebral stroke is approximately 1.1 million, which tends to increase with the aging society [1]. Furthermore, among care recipient diseases, cerebral stroke possesses the second-highest prevalence of dementia [2]. Therefore, rehabilitation for physical recovery is essential for maintaining and improving the quality of life (QoL) of patients. In this study, we focused on rehabilitation based on gait, which is a fundamental component of numerous daily activities.

The most widely used gait rehabilitation devices in facilities are crutches, parallel bars, and treadmills. Research has led to the development of many high functional treadmills. Ando et al. proposed a method using a split-type treadmill and biofeedback to improve the symmetry



(a) AFO (hanging type). (b) LOKOMAT (Hocoma Co.).

Fig. 1. Types of gait rehabilitation equipment.

of the stance phase [3]. Kikuchi et al. proposed a regulation method to achieve the optimal speed in treadmills by measuring the step length with a depth sensor [4].

Unloading body weight is essential in gait rehabilitation, specifically for hemiplegic patients, to prevent falls and reduce the burden on the legs. Many studies have reported patients falling while using crutches and parallel bars [5]. A failure during rehabilitation can reduce motivation for rehabilitation and impede learning [6]. To cope with these issues, the body hanging function and other similar devices have been commercialized, as seen in **Fig. 1** [a, b]. While hanging-type equipment can significantly prevent falls [7] and reduce the burden on the legs, they occupy large space, require time to wear, and have an introduction cost.

In this study, we propose a non-wearing-type pneumatic power-assist device for a gait rehabilitation. The proposed device can sustain the body weight of patients by pushing their armpit up at the stance phase to reduce the burden on the legs and support the pull up motion of the leg during the swing phase to promote the forward step. We quantitatively verified the effectiveness of the device through experiments.

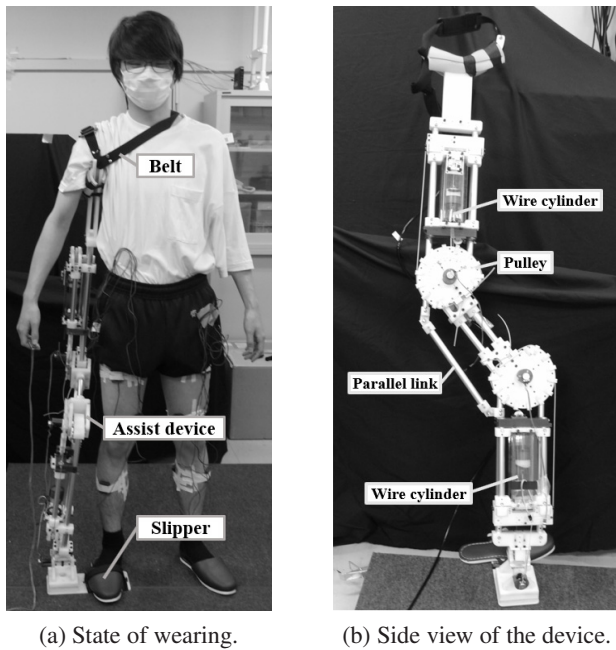


Fig. 2. Non-wearing type pneumatic power assist device.

2. Non-Wearing Type Pneumatic Power Assist Device

2.1. Overview of the Developed Device

The non-wearing-type pneumatic power assist device proposed in this study (hereinafter referred to as “the assist device”) is shown in Fig. 2. The assist device supports only one side of the subject, with the lower end fixed to the side of the wearer’s shoe and in contact with the ground, and the other end with a brace in contact with the wearer’s lower armpit [8]. An exoskeleton-type device, such as in [9], could be used as a gait assist device, however, the installation is time consuming and is large scale. The proposed assist device comes in contact with a patient at just two points and does not restrain the patient’s movements owing to the minimally invasive property of the device. Although the total weight of the device is approximately 5.0 kg, it does not become a direct burden on a wearer since it is fixed to the ground. A pneumatic actuator generates rotational torque on the waist and knee joints to lift the armpit, as seen in Fig. 2(b). Furthermore, the assist device behaves as one DOF link mechanism due to the introduction of a parallel link mechanism, as seen in Fig. 3.

In general, pneumatic cylinders are effective in wearable devices owing to their high power/weight ratio. However, because they include piston rods, they occupy large space. Therefore, we developed a wire-type pneumatic cylinder wherein the piston rod was replaced by a wire in a piston cylinder set (Airpel.co, Airpot 2K444), which drives a pulley to apply torque around each joint. The maximum rotational torque in one joint at a cylinder pressure of 450 kPa is 55.8 Nm. We aimed to sustain 50% of the patient’s body weight using the device. The average weight of a Japanese is approximately 60 kg, and in a

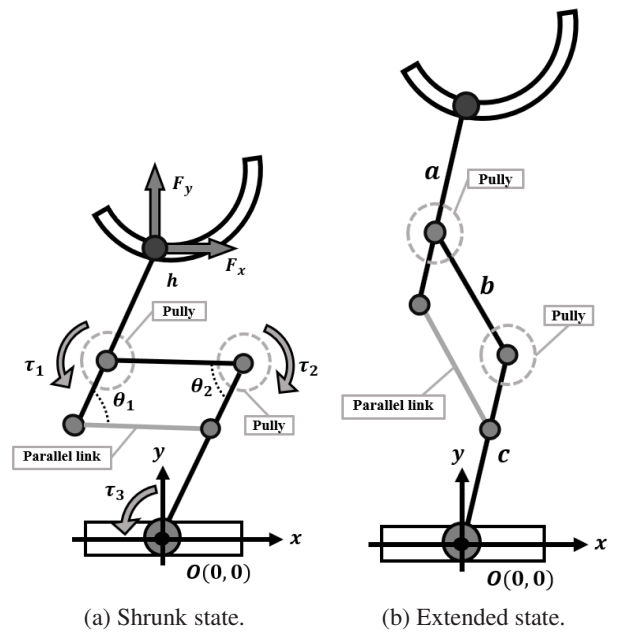


Fig. 3. Kinematic model of the assist device.

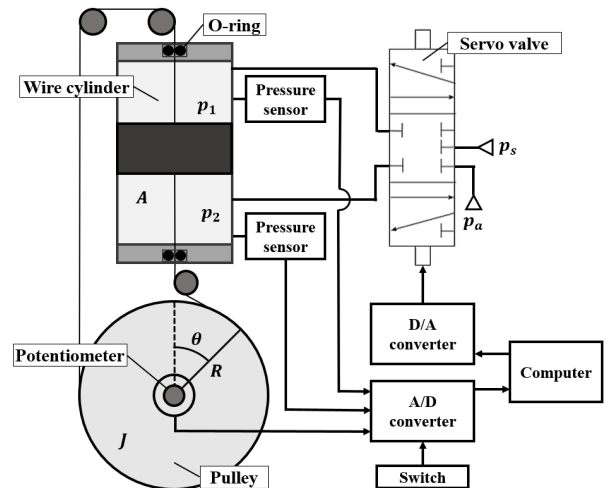


Fig. 4. Pneumatic driving circuit.

posture that supports the armpit of the patient with average height, the device can generate 530 N in the vertical direction, indicating that the device has sufficient torque generation ability.

Figure 4 shows the pneumatic driving circuit for one joint. The rotational angle of the pulley θ and pressures p_1, p_2 in the cylinder chambers, are detected using potentiometer and pressure sensors (Keyence Corp., AP-C43), respectively. A switch was used to determine the support timing in gait rehabilitation described in Section 4.3. The output voltages from the sensors were fed back to an A/D converter. A 5 port flow-type servo valve (FESTO, KMPYE-5) regulated the pressure difference $p_1 - p_2$ in the cylinder. The control system was implemented using RT-AI, a real-time extension of Linux, with a sampling period of 5 ms.

2.2. Kinematic Analysis

Figure 3 shows the kinematic model of the assist device with a base coordinate system O set at the lower end, a hand vector (relative position of the armpit from the base coordinate system) and joint vector defined as $h = [x, y]^T$ and $\theta = [\theta_1, \theta_2, \theta_3]^T$, respectively.

Forward kinematics $h = I(\theta)$ is given as follows:

$$\begin{cases} x = a \cos(\theta_1 + \theta_3 - \theta_2) - b \cos(\theta_2 - \theta_3) + c \cos \theta_3 \\ y = a \sin(\theta_1 + \theta_3 - \theta_2) + b \sin(\theta_2 - \theta_3) + c \sin \theta_3 \\ \dots \dots \dots \end{cases} \quad (1)$$

where a , b , and c are the link lengths, as seen in Fig. 3.

The average height of Japanese in their 20s to 50s is approximately 1.65 m [10], of which approximately 82% is determined as the location of an armpit [11]. Consequently, a supported position (armpit) by the assist device is approximately 1.35 m. For the manipulator to reach the support position when the piston is at the center of the cylinder, the length of each link is set as $a = 0.625$, $b = 0.3$, $c = 0.525$ m. The supported position for patients having a height different from the average height can be easily achieved by changing the link of the aluminum pipe. On introducing a parallel-link mechanism, the joint angle was constrained to $\theta_1 = \theta_2$, and the forward kinematics $h = I(\theta)$ is given as follows:

$$\begin{cases} x = a \cos(\theta_3) - b \cos(\theta_1 - \theta_3) + c \cos \theta_3 \\ y = a \sin(\theta_3) + b \sin(\theta_1 - \theta_3) + c \sin \theta_3 \end{cases} \quad (2)$$

Using a Jacobian matrix J_{aco} from the principle of virtual work, the relation between the torque vector $\tau = [\tau_1, \tau_2]^T$ around each joint and the applied force vector at the supported position $F = [F_x, F_y]^T$ can be given as:

$$\tau = J_{aco}^T F \dots \dots \dots (3)$$

By expanding Eq. (3), we acquire the statics balance equation.

$$\begin{cases} \tau_1 = a\{-F_x \sin(\theta_3) + F_y \cos(\theta_3)\} \\ \tau_2 = b\{F_x \sin(\theta_1 - \theta_3) + F_y \cos(\theta_1 - \theta_3)\} - \tau_1 \end{cases} \quad (4)$$

2.3. Required Specifications in Gait Rehabilitation

To determine the optimal support force in the stance phase, it is essential to understand the relationship between the support force and muscle activity on the affected side. However, this relationship is difficult to analyze considering that gait motion includes complicated articulated movements. Therefore, we introduced an open-source musculoskeletal simulator (OpenSim), which calculates muscle activity based on the motion data of the body and the floor reaction force, as seen in Fig. 5(a). The body size of the model was considered the same as that of a subject (adult male, 170 cm in height, and 56 kg). We first conducted data acquisition when the subject was walking. Fig. 5(b) shows the location of the markers on the subject, which were detected using a motion capture system (OptiTrack). The floor reaction force was measured by a force plate (AMTI Corp., BP400600-2000).

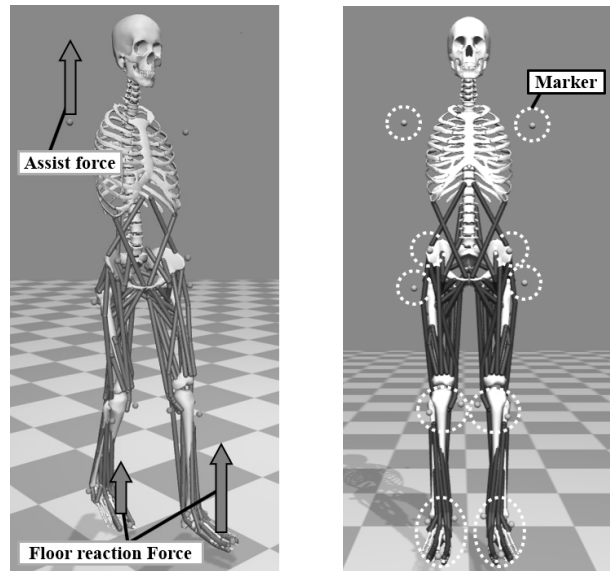


Fig. 5. Musculoskeletal simulator.

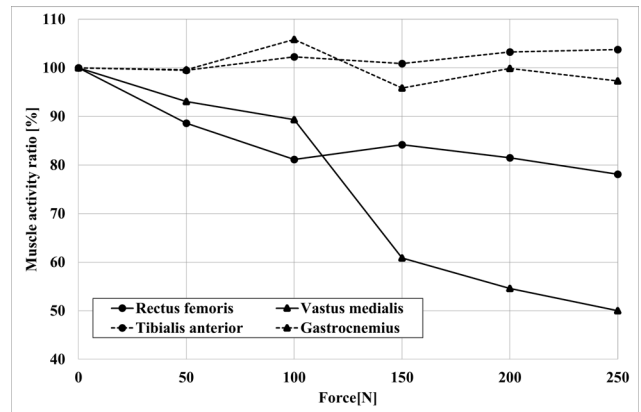
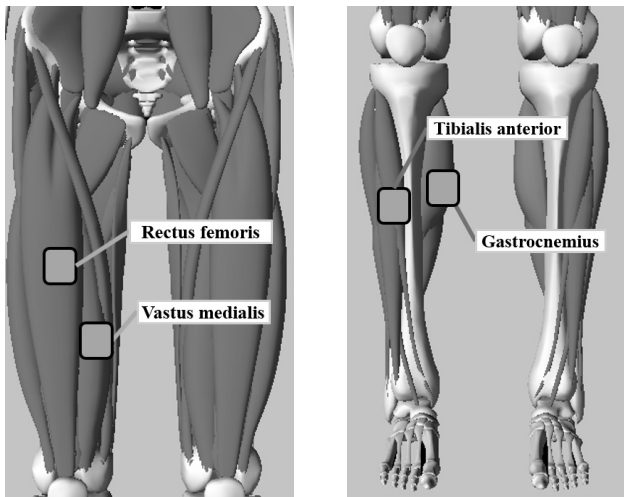


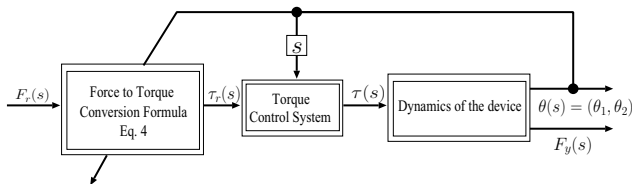
Fig. 6. Relationship between muscle burden and support force.

Next, a support force was applied to the simulation model during the stance phase to push the right-side armpit upward. The support force was constant and summed up to 250 N every 50 N. Fig. 6 shows the simulation results of the muscle activity ratio (described later in the study) against the applied support force. It was seen that the rectus femoris and vastus medialis (femur muscles), and the tibialis anterior and gastrocnemius (cruris muscles) on the right side were needed for walking, as seen in Fig. 7. The muscle activity ratio in the vertical axis indicated the percentage of the average muscle contraction force during four-step gaits without the assist device (the applied force was 0 N). Furthermore, as seen in the figure, the burden on the femur muscles decreased as the support force increased, whereas the cruris muscles were unaffected. It is worth to pay attention that muscle contraction under the applied support force was calculated using body motion data with no support force, which makes it a limited situation. However, the trend between the support force

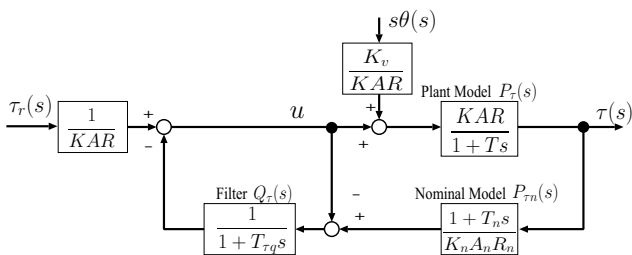


(a) Femur muscles. (b) Cruris muscles.

Fig. 7. The electrode on the dominant muscles.



(a) Complete view of the force control system.



(b) Inner torque control system.

Fig. 8. Force control system.

and muscle activity can be estimated roughly, which can contribute to the design of the reference support force depending on the patient’s condition.

3. Control System

We implemented a force control system on the assist device in this study, as seen in Fig. 8(a). In the stance phase, the patient’s armpit height was almost constant and the influence of the moment of inertia and viscosity was insignificant. Therefore, the open-loop force control without force feedback was adopted. The reference joint torque vector $\tau_r = [\tau_{r1}, \tau_{r2}]^T$ was calculated from a reference force vector $F_r = [F_{xr}, F_{yr}]^T$ using Eq. (4). As seen in Fig. 8(b), a disturbance observer was introduced in the torque control system, where, $P_\tau(s)$, $P_{\tau_n}(s)$, and $Q_\tau(s)$ are the plant, nominal model of the plant, and low-pass fil-

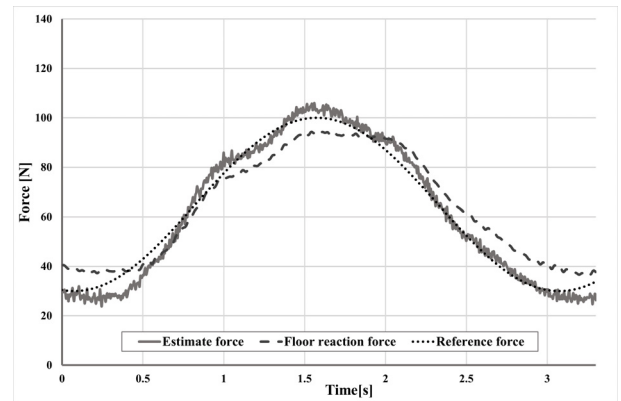


Fig. 9. Sinusoidal force control response.

ter, respectively [12]. The output of $Q_\tau(s)$ was the estimated disturbance, which includes the influence of the joint angular velocity and parameter perturbation between a plant $P_\tau(s)$ and its nominal model $P_{\tau_n}(s)$, simultaneously. If these estimated disturbances are entirely compensated, the robustness against disturbances and parameter perturbation could be improved significantly.

4. Experimental Results

4.1. Force Control Performance

Figure 9 shows the sinusoidal response of the proposed force control system, where the assist device is placed on a force plate and the top of the device pushes an aluminum frame fixed on the ground, upward. Assuming actual gait motion, the period of the reference was set to be high at 3 s. The solid line in the figure indicates the estimated force F_y determined using Eq. (4) (F_x was set to 0) based on the torque calculated using the pressure in the cylinder. The dashed line indicates the reaction force from the assist device, detected by a force plate. The force generated by the assist device follows the reference. The tracking error at the maximum value was approximately 10%, which could have been caused by a non-compensated friction force in open-loop force control. We aimed to verify the required force control accuracy in gait rehabilitation in the future.

4.2. Support Effect in a Simple Standing Situation

Before conducting gait rehabilitation, we confirmed the unloading effect of the assist device in a standing position. As seen in Fig. 10(a), a subject (healthy adult male, 170 cm in height, 53.5 kg) attached the assist device while standing using his right side, and the step-like assist force was applied at his armpit. Myoelectric sensors (Oisaka Electronics Co.) were placed as per the marker locations shown in Fig. 7. The muscles shown in Fig. 7(a) are dominant for hip and knee joint motion, and hence, were selected to verify the effect of the unloading of body weight. Similarly, the muscles shown in Fig. 7(b) con-

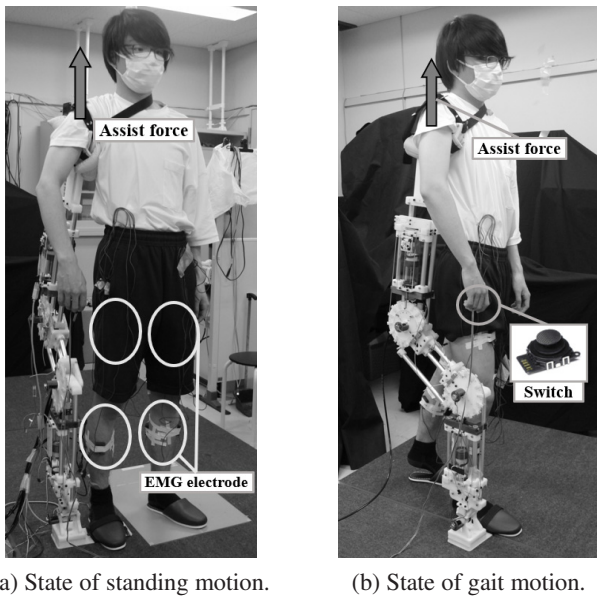


Fig. 10. Evaluation of the support effect.

tribute to ankle joint motion, and hence, were used to confirm the influence of balance in the front-back direction. The raw EMG data acquired were processed to the IEMG in Eq. (5) with an integration time $T = 0.2$ s.

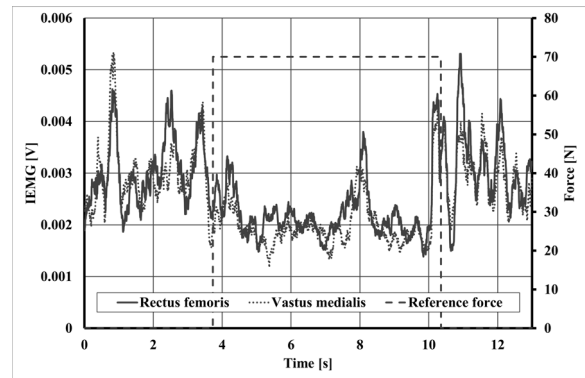
$$IEMG(t) = \frac{1}{T} \int_{t-T}^t |EMG(\tau)| d\tau \dots \dots (5)$$

Figures 11(a) and (b) show the IEMG at each femur and cruris muscle, respectively. The dotted rectangular line indicates the reference force with a step height of 70 N. When the subject's armpit was being pushed up by the assist device, the IEMG reduces, indicating that the assist device has the ability to decrease the burden on the lower body by unloading the body weight.

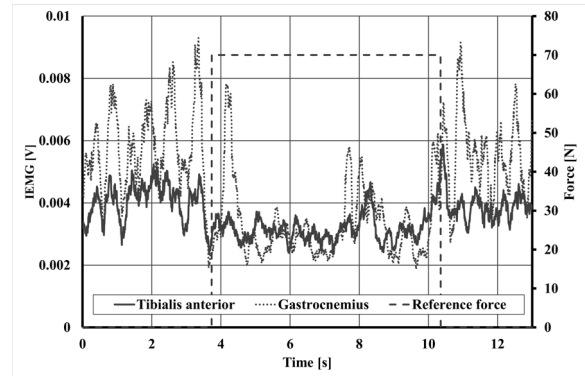
4.3. Support Effect in Gait Rehabilitation

We evaluated the support effect in gait rehabilitation. As seen in Fig. 10(a), an assist device was attached to a subject at his right side and he performed gait rehabilitation. The myoelectric sensors were placed in the same place considering the dominant muscle in gait motion, as seen in Fig. 7.

However, the support timing was an important issue. Tsuda et al. proposed a gait rehabilitation technique where the wrong use of the crutch with a tilt angle detector provided a warning to the patient [13]. Because the body moves from side to side while walking, the tilt angle detection of the support device can correspond to the support timing. However, we selected a more intuitive way of using a switch pushed by the subject during the stance phase to increase the reference force F_r in the control system up to 50 N, as seen in Figs. 8(a) and 10(b). Similarly, during the swing phase, the subject releases the switch to decrease the reference force to $F_r = -50$ N, causing the assist device to shrink. Consequently, because the device hangs from the shoulder of the subject, his right foot is



(a) Femur muscles.



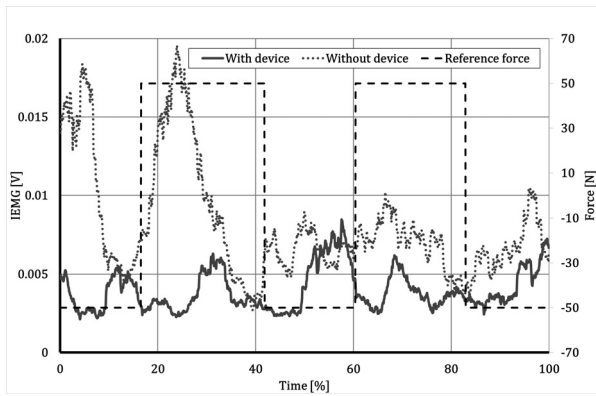
(b) Cruris muscles.

Fig. 11. The IEMG in standing motion rehabilitation.

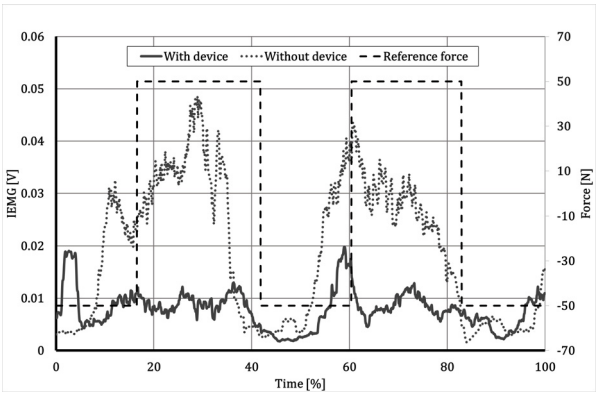
lifted up by the device, making it easier to take a step forward, even in hemiplegic patients. The physical burden from the hanging device on the shoulder during the swing phase can be decreased by installing a belt on the healthy side, as seen in Fig. 2(a).

Two healthy adult males (169 ± 0.5 cm in height and 54 ± 1 kg in weight) were chosen as subjects, and three trials were conducted. Figs. 12 and 13 show the experimental results for subjects A and B, respectively. In both figures, (a)–(d) show the IEMG of the rectus femoris, vastus medialis, tibialis anterior, and gastrocnemius muscles, respectively, as shown in Fig. 7. The horizontal axis represented the normalized time for the two-step walking period. The two upper and two lower figures indicate the cases of the femur and cruris muscles, respectively.

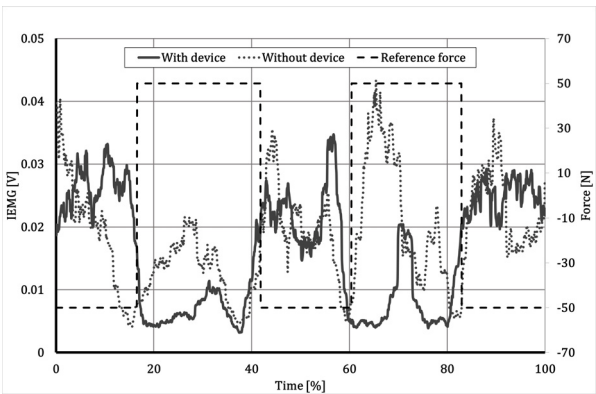
Figure 14 summarizes the experimental results of the three trials conducted with two subjects, where the average IEMG value and distribution are depicted as bar graphs. The case without the assist device was set as the standard (100%). It was observed that when a support device was used, the muscle activity ratio for the rectus femoris decreased with a significant difference in 5%, which is also confirmed by the time-domain graphs in Figs. 12(a) and 13(a). Furthermore, a decrease in muscle activity during the stance phase indicated a decrease in the burden on the upper leg and during the swing phase indicated that the leg was being lifted by the support device owing to the shrinking of the device, showing the possibil-



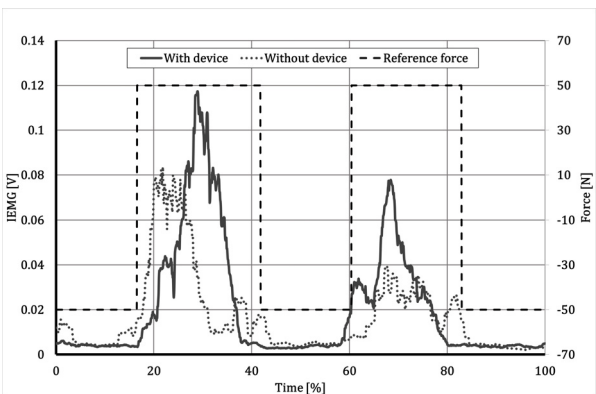
(a) Rectus femoris.



(b) Vastus medialis.

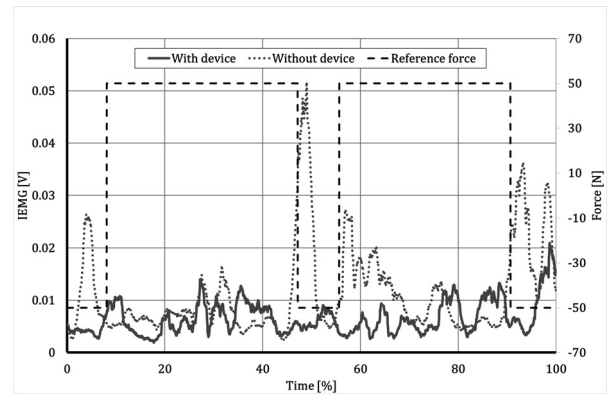


(c) Tibialis anterior.

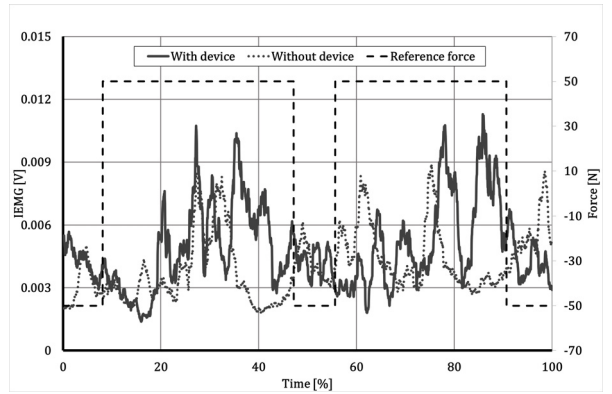


(d) Gastrocnemius.

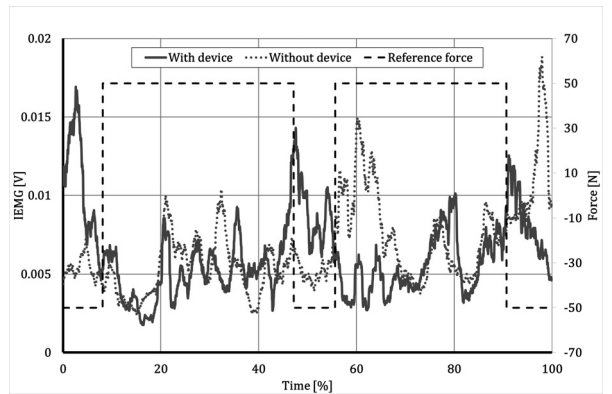
Fig. 12. Muscle burden of subject A.



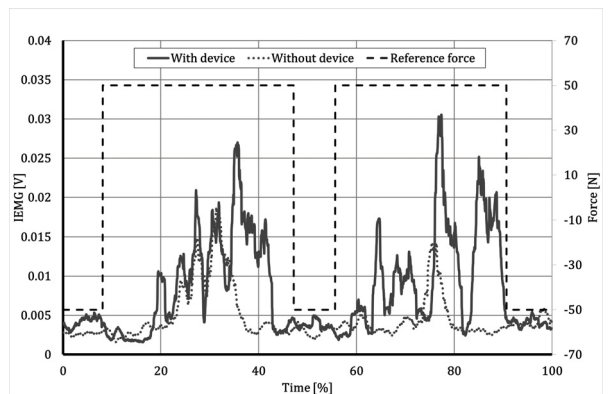
(a) Rectus femoris.



(b) Vastus medialis.



(c) Tibialis anterior.



(d) Gastrocnemius.

Fig. 13. Muscle burden of subject B.

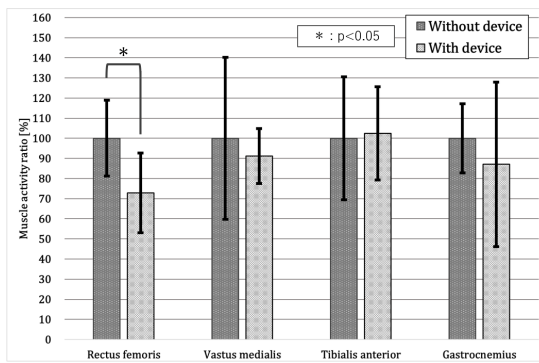


Fig. 14. Comparison of muscle activation.

ity for the hemiplegic patient to take a forward step easily. The decline in the activity of the rectus femoris in case of support can be explained by its role in the body. The rectus femoris is a biarticular muscle that assists in the movement of the hip and knee joints, which contributes to standing against gravity and knee extension during the swing phase. Therefore, a significant decrease in burden is observed when the body weight is unloaded and swing motion is supported. As seen in Fig. 13(b), the activity of the vastus medialis was not decreased compared to that in Fig. 12(b) considering the assumption that subject B walked with his knee joint extended as usual during the stance phase by shifting his body weight to the opposite side of the device. The result shows that it is necessary for patients to deposit their weight on the device.

As seen in Fig. 14, the other two muscles, tibialis anterior and gastrocnemius, showed no significant statistical difference assuming that the subjects tried to maintain body balance, considering these two muscles are dominant for maintaining body balance in front and back directions. The results showed the same tendency as that in Fig. 6, suggesting that although the support device can unload the body weight, the patient's body balance must be cared for by a physiotherapist. However, the burden on the physiotherapist decreases considering the patient's weight could be ignored.

5. Conclusions

In this study, we proposed a gait rehabilitation system based on a non-wearing-type pneumatic power assist device that can unload body weight by pushing a patient's armpit upward. Before conducting the gait rehabilitation experiment, we introduced a musculoskeletal simulator to verify the relationship between the support force applied by the device and muscle activity. The results are useful for setting the reference support force.

In actual gait rehabilitation, the IEMG of the rectus femoris muscle decreases in both the stance and swing phases. It is because the assist device unloaded the patient's weight during the stance phase, and lifted up the leg during the swing phase by shrinking the link, which indi-

cates that even a hemiplegic patient would be able to step forward easily. For the vastus medialis muscle, one subject showed no significant effect, which could be because he walked with his knee joint extended during the stance phase as usual by shifting the body weight to the opposite side of the device. This result suggests that the patient is required to be familiar with using the device. For another muscle in the leg, except for the rectus femoris and vastus medialis, almost no effect was confirmed. Because these muscles are dominant in maintaining body balance, these experimental results indicate that the body balance must be cared for by a physiotherapist.

The proposed assist device should prevent the patient's armpit from squeezing, considering nerves and blood vessels pass through the armpit [14, 15]. Therefore, for future research, we will consider improving the material and shape of the brace mounted on the top of the assist device from a view of the distribution of body pressure.

Acknowledgements

This work was supported by JSPS KAKENHI Grant Number JP20K04400.

References:

- [1] Ministry of Health, Labor and Welfare, "Annual Health, Labour and Welfare Report," 2018 (in Japanese).
- [2] Ministry of Health, Labor and Welfare, "Comprehensive Survey of Living Conditions," 2019 (in Japanese).
- [3] T. Ando, E. Ohki, Y. Nakashima, Y. Akita, H. Iijima, O. Tanaka, and M. G. Fujie, "Pilot Study of Split Belt Treadmill Based Gait Rehabilitation System for Symmetric Stroke Gait," *J. Robot. Mechatron.*, Vol.24, No.5, pp. 884-893, 2012.
- [4] T. Kikuchi, K. Sakai, and K. Ishiya, "Gait Analysis with Automatic Speed-Controlled Treadmill," *J. Robot. Mechatron.*, Vol.27, No.5, pp. 528-534, 2015.
- [5] Ministry of Health, Labor and Welfare, "Important case summary information," 2003 (in Japanese).
- [6] C. Okaniwa, H. Yamasaki, M. Kato, H. Asuma, and A. Kitahara, "Standing and Gait Training in Hemiplegic Patients with Pusher Sign – The approach using the physical guidance and fading method –," *J. of Kochi Rehabilitation Institute*, Vol.7, pp. 55-60, 2006.
- [7] Japanese Society of Physical Therapy, "Physical therapy guidelines First Edition," 2011 (in Japanese).
- [8] M. Yokota and M. Takaiwa, "Development of Non-Wearing Type Pneumatic Power Assist Device – Basic Concept and Performance Evaluation –," *J. Robot. Mechatron.*, Vol.32, No.5, pp. 1052-1060, 2020.
- [9] J. F. Veneman, R. Kruidhof, E. E. G. Hekman, R. Ekkelenkamp, E. H. F. van Asseldonk, and H. van der Kooij, "Design and Evaluation of the LOPES Exoskeleton Robot for Interactive Gait Rehabilitation," *IEEE Trans. on Neural Systems and Rehabilitation Engineering*, Vol.15, No.3, pp. 379-386, 2007.
- [10] Ministry of Health, Labor and Welfare, "National Health and Nutrition Survey Report," 2017 (in Japanese).
- [11] D. B. Chaffin and G. B. J. Andersson, "Occupational Biomechanics," Wiley, 1984.
- [12] M. Takaiwa and T. Noritsugu, "Positioning control of pneumatic parallel manipulator," *Int. J. Automation Technol.*, Vol.2, No.1, pp. 49-55, 2008.
- [13] N. Tsuda, A. Ito, M. Tounai, and Y. Nomura, "Development of Axillary Crutch Walking Trainer for Three-Point Gait," *Trans. of the Japanese Society for Medical and Biological Engineering*, Vol.47, No.2, pp. 209-214, 2009 (in Japanese).
- [14] D. M. Bauer, D. C. Finch, K. P. McGough, C. J. Benson, K. Finstuen, and S. C. Allison, "A comparative analysis of several crutch-length-estimation techniques," *Phys. Ther.*, Vol.16, No.3, pp. 294-300, 1991.
- [15] I. T. Chang and A. D. Hohler, "Bilateral radial nerve compression (crutch palsy): a case report," *J. of Neurology & Neurophysiology*, Vol.3, Issue 3, 1000130, doi: 10.4172/2155-9562.1000130, 2012.

Supporting Online Materials:

- [a] Data sheet of AFO (hanging type) SAKAI Medical Co. <https://www.sakaimed.co.jp/rehabilitation/exercise-therapy/standingwalkingtraining/unweighingsystemnxstep/> [Accessed February 20, 2021]
- [b] Data sheet of Lokomat Hocoma Co. <https://www.hocoma.com/solutions/lokomat/> [Accessed February 3, 2021]



Name:
Masashi Yokota

Affiliation:
Ph.D. Course Student, Graduate School Advanced Technology and Science, Tokushima University

Address:

2-1 Minamijyousanjima-cho, Tokushima 770-8506, Japan

Brief Biographical History:

2019 Received Master's degree from Shizuoka Institute of Science and Technology

2019- Ph.D. Course Student, Tokushima University

Main Works:

- "Development of Non-Wearing Type Pneumatic Power Assist Device – Basic Concept and Performance Evaluation –," J. Robot. Mechatron., Vol.32, No.5, pp. 1052-1060, 2020.

Membership in Academic Societies:

- The Japan Society of Mechanical Engineers (JSME)
 - The Japan Fluid Power System Society (JFPS)
 - Society of Automotive Engineers of Japan (JSAE)
-



Name:
Masahiro Takaiwa

Affiliation:
Professor, Graduate School of Technology, Industrial and Social Sciences, Tokushima University

Address:

2-1 Minamijyousanjima-cho, Tokushima 770-8506, Japan

Brief Biographical History:

1992- Associate Researcher, Okayama University

2000- Lecturer, Okayama University

2007- Associate Professor, Okayama University

2015- Professor, Tokushima University

Main Works:

- "Fingertip Force Displaying Device Using Pneumatic Negative Pressure," Int. J. Automation Technol., Vol.8, No.2, pp. 208-215, 2014.
- "Wrist Rehabilitation Simulator for P.T. Using Pneumatic Parallel Manipulator – Regulation of Wrist Viscoelastic Property and Therapy Motion Evaluation –," Proc. of the 10th JFPS Int. Symp. on Fluid Power, 2B15, 2017.
- "Development of Finger-Wrist Rehabilitation Device Using Pneumatically Driven Parallel Sticks," J. Robot. Mechatron., Vol.32, No.5, pp. 1044-1051, 2020.

Membership in Academic Societies:

- The Japan Society of Mechanical Engineers (JSME)
 - The Japan Fluid Power System Society (JFPS)
 - The Robotics Society of Japan (RSJ)
 - The Virtual Reality Society of Japan (VRSJ)
 - The Society of Instrument and Control Engineers (SICE)
-